

Analogue Gravity and ultrashort laser pulse filamentation.

D. Faccio¹, S. Cacciatori², V. Gorini², V.G. Sala¹, A. Averchi¹, A. Lotti¹, M. Kolesik³, J.V. Moloney³

¹*CNISM and Department of Physics and Mathematics,*

Università dell'Insubria, Via Valleggio 11, I-22100 Como, Italy

²*Department of Physics and Mathematics, Università dell'Insubria, Via Valleggio 11, I-22100 Como, Italy*

³*Arizona Center for Mathematical Sciences and Optical Sciences Center,*

University of Arizona, Tucson, 85721 AZ, U.S.A

(Dated: November 10, 2018)

Ultrashort laser pulse filaments in dispersive nonlinear Kerr media induce a moving refractive index perturbation which modifies the space-time geometry as seen by co-propagating light rays. We study the analogue geometry induced by the filament and show that one of the most evident features of filamentation, namely conical emission, may be precisely reconstructed from the geodesics. We highlight the existence of favorable conditions for the study of analogue black hole kinematics and Hawking type radiation.

PACS numbers: 190.5940, 320.2250

The persistent lack of a satisfactory quantum model of gravity has led to the development of a semiclassical approach in which the dynamics of a quantum field is analyzed in the curved spacetime metric determined by the classical gravitational field [1]. One of the most intriguing predictions of the semiclassical model is the thermalization of the quantum field in the presence of the event horizon of a black hole [2]. However, it turns out that for a typical stellar mass black hole the temperature of this expected radiation is so low (~ 10 nK) and the intensity of the latter far away from the actual source is so weak as to be extremely unlikely to ever be detected. On the other hand, Unruh proposed the use of gravity analogue systems that reproduce the kinematics of gravitational systems as a means to gain insight and experimental verification of gravitational theories in earth-based laboratories [3]. A number of analogue systems have been proposed, relying mainly on acoustic perturbations in low-temperature condensates and on light rays in a moving dielectric [4, 5]. These mostly suffer from the same limitation of astrophysical black holes, i.e. extremely low Hawking temperatures, and therefore continue to pose a strong experimental challenge. More recently Philbin et al. proposed a dielectric medium based analogue in which a fiber soliton generates, through the nonlinear Kerr effect, a refractive index perturbation (RIP) which modifies the space-time geometry as seen by co-propagating light rays [6]. The Hawking temperature in the laboratory reference frame is found to be given by $kT = \hbar\alpha/2\pi c$ where the surface gravity $\alpha = -(c/\delta n)\partial\delta n/\partial\tau$ is determined by the variation of the RIP along the retarded time coordinate τ .

Ultrashort laser pulse filamentation in bulk dispersive media with Kerr nonlinearity is characterized by the transformation of an input bell-shaped laser pulse into a tightly focused, high intensity peak that may propagate sub-diffractively over distances much larger than the Rayleigh length [7]. One of the most spectacular manifestations of filamentation is conical emission, i.e. the generation of new wavelengths propagating along a cone

with the cone angle typically increasing with increasing wavelength shift from the pump pulse. A further important feature of filamentation that is relevant for what follows is the typical pulse splitting process that leads to the formation of two daughter pulses, one traveling slightly slower, the other slightly faster than the input Gaussian pulse.

In this letter we present a dielectric analogue based on the RIP induced by ultrashort laser pulse filamentation. We analyze in detail the light-ray geodesics predicted for such a system and show that these lead to a conical emission that is described by the same relation predicted by other models. This is verified experimentally in the present work both for a narrow bandwidth probe pulse and for a spectrally broad pulse. In the latter case a blue-shifted and a red-shifted spectral peak appear and this is interpreted as evidence of the complex Doppler effect [8, 9]. Finally we propose possible operating conditions for the observation of Hawking radiation.

We start by analyzing how the filament modifies the effective space-time geometry as seen by light rays. The intense core of the filament excites, through the nonlinear Kerr effect, a refractive index profile $n(x, y, z, t) = n_0 + \delta n(x, y, z, t)$ where $\delta n(x, y, z, t) = n_2 I(x, y, z, t)$, n_2 is the nonlinear Kerr coefficient and $I(x, y, z, t)$ is the intensity profile of the filament light pulse. We note that here z is the pulse longitudinal coordinate directed along the propagation direction and t is the time in the laboratory reference frame. The analogue space-time metric in the laboratory reference frame is

$$ds^2 = \frac{c^2}{n(x, y, z, t)^2} dt^2 - dx^2 - dy^2 - dz^2 = g_{\mu\nu} dx^\mu dx^\nu. \quad (1)$$

Note that this is not the metric describing the light propagation in a moving medium, see [10]. This is because, in our case, even though the index profile is moving, the dipoles constituting the medium are at rest in the laboratory. The null geodesics in the laboratory reference frame are the solutions of the geodesic equation $\ddot{x}^\mu + \Gamma_{\nu\sigma}^\mu(x(\lambda))\dot{x}^\nu \dot{x}^\sigma = 0$ with

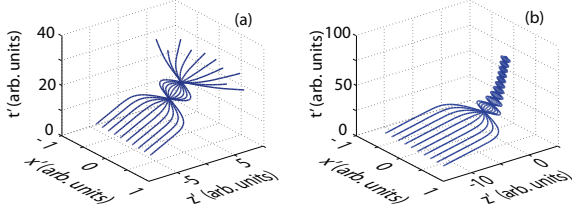


FIG. 1: (a) Space-time light ray geodesics in the reference frame of the moving RIP. (a) corresponds to a subluminal RIP: the light rays catch up with the RIP and the geodesics are deformed from the initial “straight” propagation. After two refocusing cycles (the details depend on the initial conditions) the light rays finally escape from the RIP with modified angles and frequencies. (b) corresponds to an RIP with $v = c/(1 + \delta n_0)$: the light rays are now trapped by the RIP event horizon and cannot escape. The increasing steepness of the curves as they approach $z=0$ tells us that light is grinding to a halt inside the RIP.

$g_{\mu\nu}(x(\lambda))\dot{x}^\mu(\lambda)\dot{x}^\nu(\lambda) = 0$ and $\Gamma_{\nu\rho}^\mu = (1/2)g^{\mu\sigma}[\partial_\nu g_{\sigma\rho} + \partial_\rho g_{\sigma\nu} - \partial_\sigma g_{\nu\rho}]$. Figure 1(a) shows the calculated geodesics in the RIP co-moving reference frame, considering a refractive index perturbation profile in the form of a Gaussian, $\delta n = \delta n_0 \exp[-(z - vt)^2 - x^2 - y^2]$. The RIP bends the geodesics toward its center and introduces also a time deformation. This leads to a simultaneous modification of the light ray propagation angle θ and frequency, ω . These effects are best studied in (θ, ω) space. We start from the incoming light ray wavevector which may be written in the RIP co-moving reference frame as $k_{\text{in}} = (k_{\text{in}}^0, 0, 0, k_{\text{in}}^z)$. The spacetime metric experienced by the observer co-moving with the filament is

$$\begin{aligned} ds^2 &= c^2 \left(1 + \left[\frac{1}{n^2} - 1 \right] \gamma^2 \right) dt'^2 + 2\gamma^2 v \left[\frac{1}{n^2} - 1 \right] dt' dz' \\ &\quad - \left(1 - \left[\frac{1}{n^2} - 1 \right] \gamma^2 \frac{v^2}{c^2} \right) dz'^2 - dx'^2 - dy'^2 \\ &= g'_{\mu\nu} dx'^\mu dx'^\nu, \end{aligned} \quad (2)$$

where $\gamma = 1/\sqrt{1 - (v/c)^2}$.

Note that in this frame the metric is stationary, being independent from the coordinate t' . Then, time translations are symmetries and determine a conserved quantity: $E = k'^\mu \xi'^\nu g'_{\mu\nu}$, where $\xi' = (1, 0, 0, 0)$ is the associated Killing vector. Thus $E = k'^\mu g'_{\mu 0} = k'_0$ and $E_{\text{out}} = E_{\text{in}}$ is equivalent to

$$k'_{0\text{out}} = k'_{0\text{in}}. \quad (3)$$

In other words in the comoving frame the frequency is constant along a geodesic, as expected ($\omega' = ck'_0$). Turning back to the laboratory frame, where $k_{\text{in}} = (k_{0\text{in}}, 0, 0, -k_{\text{in}}^z)$ and $k_{\text{out}} = (k_{0\text{out}}, -k_{\text{out}}^x, -k_{\text{out}}^y, -k_{\text{out}}^z)$, equation (3) becomes

$$k_{\text{out}}^z = k_{\text{in}}^z + \frac{\omega_{\text{out}} - \omega_{\text{in}}}{v}. \quad (4)$$

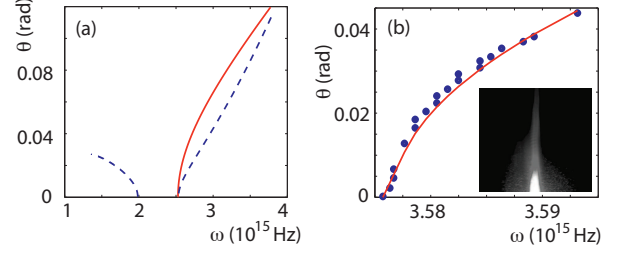


FIG. 2: (θ, ω) spectrum of the scattered light rays calculated from Eq. (4). (a) solid line - neglecting material dispersion (equivalent to the standard Doppler effect), dashed line - including material dispersion (equivalent to the complex Doppler effect). (b) Measured spectral deformation of a probe pulse in the presence of a filament. Circles - experimental maximal intensity points taken from the measurement shown in the inset. Solid line - fit obtained using Eq. (4) neglecting material dispersion.

Finally, the (θ, ω) distribution of the outgoing light rays as measured in the laboratory reference frame is given by inserting Eq. (4) in $\theta \simeq k_\perp/k(\omega) = \sqrt{1 - [k_{z\text{out}}/k(\omega)]^2}$ where $k(\omega)$ is the material dispersion relation. We underline that this last equation, along with Eq. (4), is identical to that derived within the framework of the Effective-Three-Wave-Mixing (ETWM) and X-wave models that have been successfully used to describe the main spectral features and dynamics of ultrashort laser pulser filamentation [11, 12, 13, 14, 15, 16]. The present derivation of these relations on the one hand lends further support and understanding to these interpretations of dynamics in nonlinear optics. On the other hand, it justifies our analogue model as a candidate to study the analogue gravity. It is also important to note that Eq. (4) has been derived under the approximation of negligible material dispersion *within* the RIP. We have verified that this approximation is valid as long as the difference between the RIP velocity, v and the material group velocity, $v_g = dk/d\omega$, is small. A more detailed discussion regarding this point will be given in a future publication but, as verified below, filamentation is indeed characterized by $|(v - v_g)/v_g| \ll 1$, thus justifying our derivation.

We underline that one of the cardinal points in deriving Eq. (4) is the Doppler shift that allows to transform back and forth between the two reference systems. On the basis of this, two different regimes may be highlighted depending on how one accounts for the material dispersion in the medium surrounding the RIP. If we neglect the material dispersion, i.e. $k(\omega) = \omega n(\omega_{\text{in}})/c$ we obtain the solid curve in Fig. 2(a). This is equivalent to the standard Doppler effect in which observers at an angle with respect to the direction of motion of a scatterer experience a sweep in the scattered frequency. However, along the line of motion, no frequency shift in the *forward* direction is observed. Conversely, we may fully account for material dispersion, i.e. $k(\omega) = \omega n(\omega)/c$. In this case we obtain the dashed curve in Fig. 2(a). This is equivalent

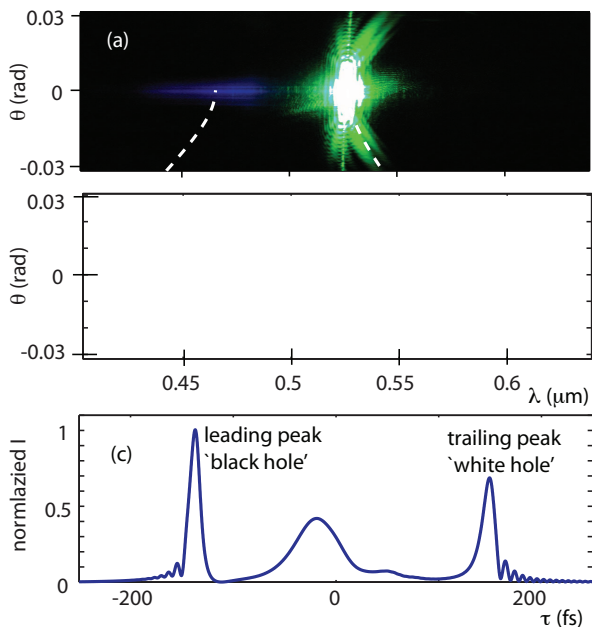


FIG. 3: (θ, λ) spectra of filament pulses in a 3 cm fused silica sample. (a) input energy = 1.5 μJ , (b) input energy = 1.8 μJ . The dashed lines correspond to the spectral supports predicted by Eq. (4), including material dispersion and with (a) $v = 0.996c/n_g$ and (b) $v = 1.0032c/n_g$, $v = 0.997c/n_g$. (c) numerically simulated temporal profile of the filament.

to the so-called complex Doppler effect [8] in which the emitter is seen to emit two (or more) frequencies along the direction of motion. Indeed, in the presence of dispersion the Doppler formula $\omega' = \gamma\omega[1 - vk(\omega)]$, which lies at the basis of the coordinate transformations used in deriving Eq. (4), may have two or more solutions depending on the complexity of the $k(\omega)$ dispersion relation [8, 9].

We experimentally verified these findings. Experiments were carried out using a regeneratively amplified Nd:Glass laser delivering pulses at 10 Hz repetition rate with 1 ps pulse duration and 1055 nm central wavelength (Twinkle, Light Conversion Ltd., Lithuania). The nonlinear Kerr medium was a 2 cm long fused silica sample. A filament was generated by focusing down to a 100 μm input diameter a pulse with an input energy of 20 μJ . A second probe pulse is obtained by loosely focusing (1 mm diameter) 100 nJ at the second harmonic wavelength, thus allowing to easily distinguish the pump and probe pulses. This allows one to easily separate the filament and probe pulses at the sample output. In Fig. 2(b) the solid circles show points of maximal intensity taken from the measured output probe spectrum (shown in the inset). Due to the limited spectral bandwidth of the probe pulse we may effectively neglect material dispersion and thus obtain a good fit for the data with Eq. (4), using $k(\omega) = \omega n(\omega_{\text{in}})/c$.

In order to test the validity of Eq. (4) in the presence of material dispersion we performed a second set of exper-

iments in which the pulse probing the RIP is the same pump pulse generating the filament. It is well-known that filamentation will lead to pulse splitting and to significant pulse shortening [7]. Starting from an input 200 fs pump pulse at the second harmonic of our laser, i.e. at 527 nm, the filament dynamics lead to pulse durations as short as 20-30 fs with correspondingly broad spectral bandwidths. The input pulse was focused to a 100 μm diameter at the input of a 3 cm long fused silica sample. By carefully controlling the input energy it was possible to shift the onset of filamentation toward the end of the sample so that only a very short filament was observed before the pulse exited into air, thus quenching all nonlinear effects and subsequent interactions. In this way we avoid the relatively intense on-axis frequency continuum generated by long-scale filaments that would completely cover the spectral features that we are aiming to unveil. Figure 3(a) shows the measured spectrum with an input energy of 1.5 μJ . The input Gaussian pump pulse spectrum has been reshaped by the RIP and exhibits marked red-shifted conical emission tails and a new blue-shifted component, mainly concentrated around $\theta = 0$. The dashed lines show the spectral support predicted from Eq. (4) with $v = 0.996c/n_g$ where $n_g = c/v_g$ is the material group index at 527 nm. The observed spectral features are well reproduced by the curve and we may thus interpret the spectrum as a manifestation of the complex Doppler effect by which the input 527 nm pulse is scattered by an RIP that is traveling slightly slower than the input Gaussian pulse. We note that a similar blue-shifted peak has been previously reported [17] and was shown to be related to a steep trailing front within the filament. This is also in keeping with the results and interpretation of Philbin et al., who assimilates a trailing pulse edge to a white hole [6]. Such a white hole will indeed blue-shift any incoming light rays, as also observed in our measurement.

Figure 3(b) shows the measured spectrum with a slightly higher input energy of 1.8 μJ . Now, in addition to the blue-shifted peak, we also observe a red-shifted peak. As before, the dashed lines show the spectral support predicted from Eq. (4), with $v = 0.997c/n_g$ for the blue-shifted spectrum and with $v = 1.0032c/n_g$ for the red-shifted spectrum. The fact that the blue peak may appear independently of the red peak excludes four-wave-mixing as the generating process. We thus interpret the on-axis red peak as the result of the complex Doppler effect for light rays scattered from a leading front in the filament. This leading front is just a time-reversed realization of the trailing front analyzed in Fig. 3(b) and it may thus be assimilated to a black hole [6]. In Fig. 3(c) we show the numerically calculated intensity profile of the pulse along the propagation axis at the sample output. A description of the numerical code is given in [11, 18, 19] and a detailed comparison with experiments is given in [17]. As can be seen, the pulse is indeed characterized by a sharp trailing edge, that gives rise to a blue-shifted spectral peak, and by an equivalently sharp leading edge

that gives rise to red-shifted spectral peak. For different input energies the filament dynamics may change significantly and only a trailing pulse (and blue shifted spectral peak) may be observed [17], thus explaining the difference between Figs. 3(a) and (b). We note that for a pulse propagating in nonlinear media with a positive Kerr coefficient, the formation of a shock front on the trailing edge is to be expected and has been frequently reported [20, 21]. However the formation of a leading shock front is not as obvious and indeed is a peculiar feature of filamentation [22]. This aspect makes filamentation particularly suited to the study of what concerns the present work.

We underline once more that in order to actually observe Hawking radiation the RIP should travel superluminally with respect to the phase velocity of the incoming light rays. Figure 1(b) shows the geodesics in the co-moving RIP reference frame in the limiting case for the horizon event formation, i.e. for an RIP velocity equal to the light phase velocity. The geodesics are now strongly deformed and, as light gradually grinds to a halt, cannot escape from the RIP. From the experimental viewpoint, Fig. 3(c) shows how the filament pulse (and thus also the corresponding RIP) consists of two main peaks, with the trailing peak being slower and the leading peak faster than the input pulse. It has been shown that by correctly choosing the input pulse conditions in function of the spe-

cific Kerr medium, it is possible to create a leading pulse that is superluminal even with respect to the same input carrier frequency [23]. Such an RIP will therefore appear as a black hole for the pump pulse carrier frequency.

In conclusion we have described the space-time geometry of light rays in the presence of a filament. The equations predict a specific shape for the aberrated light rays that has been confirmed experimentally. The results indicate the presence of both white and black hole horizons. Using the same formulas of [6], a 5 fs pulse at 800 nm (2 optical cycles) will lead to a Hawking temperature corresponding to a peak wavelength around 1.2 μm for which high sensitivity detectors are readily available. One may envision other possibilities for achieving superluminal pulses in Kerr media such as the use of Bessel-like pulses, although filaments maintain a certain attractiveness due to the spontaneous pulse shortening and the possibility to observe more exotic phenomena such as black hole lasing [24, 25].

The authors acknowledge measurements performed in the Ultrafast Nonlinear Optics Laboratory, Università dell'Insubria, Como, Italy, led by Prof. Paolo Di Trapani. JVM acknowledges support from US Air Force Office of Scientific Research (AFOSR) under contract FA9550-07-1-0010.

-
- [1] N. D. Birrell and P. C.W. Davies, *Quantum Fields in Curved Space*, (Cambridge University Press, Cambridge, England, 1984).
- [2] S.W. Hawking, *Commun. Math. Phys.* **43**, 199 (1975).
- [3] W. G. Unruh, *Phys. Rev. Lett.* **46**, 1351 (1981).
- [4] *Artificial Black Holes*, edited by M. Novello et al. (World Scientific, Singapore, 2002).
- [5] C. Barceló et al., *Living Rev. Relativity* **8**, 12 (2005), <http://www.livingreviews.org/lrr-2005-12>.
- [6] T.G. Philbin et al., *Science*, **319**, 1367 (2008).
- [7] A. Couairon et al., *Phys. Rep.* **441**, 47 (2007).
- [8] I.M. Frank, *Science*, **11**, 131 (1960), *The Nobel Lecture*.
- [9] Yu M. Sorokin, *RadioPhys. Quantum Electron.*, **36**, 410 (1993).
- [10] U. Leonhardt et al., *Phys. Rev. A* **60** (1999) 4301.
- [11] M. Kolesik, et al., *Opt. Express*, **13**, 10729 (2005).
- [12] D. Faccio et al., *Opt. Express*, **15**, 13077 (2007)
- [13] M. Kolesik et al., *Phys. Rev. Lett.*, **92**, 253901 (2004).
- [14] C. Conti, *Phys. Rev. E* **70**, 046613 (2004).
- [15] D. Faccio et al., *Phys. Rev. Lett.* **96**, 193901 (2006).
- [16] A. Averchi et al., *Opt. Lett.* **33**, 3028 (2008)
- [17] D. Faccio et al., *Phys. Rev. A*. **78**, 033825 (2008).
- [18] M. Kolesik et al., *Phys. Rev. Lett.* **89**, 283902 (2002).
- [19] M. Kolesik and J. V. Moloney, *Phys. Rev. E* **70**, 036604 (2004).
- [20] F. DeMartini et al., *Phys. Rev.* **164**, 312 (1967)
- [21] R.R. Alfano, *The Supercontinuum Laser Source*, Springer-Verlag, New York (1989).
- [22] F. Bragheri et al., *Phys. Rev. A*, **76**, 025801 (2007)
- [23] D. Faccio et al., *Opt. Express*, **16**, 11103 (2008)
- [24] S. Corley et al., *Phys Rev D*, **59**, 124011 (1999)
- [25] U. Leonhardt et al., in *Quantum Analogues: From Phase Transitions to Black Holes and Cosmology*, Springer, Berlin (2007)